Thermal-Hydraulics Analysis of A New Core-Moderator Assembly Design for the Penn State Breazeale Reactor Using the ANSYS Fluent Code

D. Uçar,[1] K. Ünlü,[1,2] B. J. Heidrich[1]

Service Provided: Penn State Breazeale Reactor

Sponsors: The Penn State Radiation Science and Engineering Center

Introduction

The Penn State Breazeale Reactor (PSBR), a TRIGA Mark-III design, is an open-pool type reactor that is cooled by the natural circulation of the demineralized and filtered water. The reactor core operates at a depth of ~5.5 m (18 ft) in the reactor pool, which has dimensions of 9.14 m in length, 4.27 m in width and 7.21 m in depth, and at a pressure of ~1.5 atm. The driving force for the natural circulation of the water is the heat generation within the fuel rods. The PSBR operates in the subcooled nucleate boiling region above 250 kW power since the temperature of the fuel rod outer is sufficiently higher than the saturation temperature of the water at the reactor's local operating pressure. Additionally, the reactor is licensed for two modes of operation: (1) the normal mode of operation with up to 1 MW nominal power and (2) the pulse mode of operation with up to 2000 MW and a pulse half width of 10 to 20 msec.

The PSBR has some inherent design issues that limit the experimental capability of the facility, such that only two of the seven available neutron beam ports can be coupled with the reactor core for experimental purposes. In addition, neutron beams in the available beam ports have a severe prompt gamma-ray component because of the current configuration of the core and the moderator tank. The limitations of the existing reactor have been discussed and analyzed in several studies [1][2][3] and the major problem was identified as the existing core-moderator assembly configuration [4]. Thus, a new-core moderator assembly has been designed and analyzed for the reactor to overcome these design problems and to increase the neutronic performance of the beam port facilities. A crescent-shaped moderator tank is favored in the new design because of the ease of coupling with the new reactor core and the beam ports. The crescent-shaped moderator tank, which has an outer diameter of 76.2 cm around the core center (centre thimble) in the optimal configuration, allows simultaneous utilization of five neutron beam ports. Furthermore, the new core-moderator assembly design minimizes the pool water around the reactor core in order to diminish the prompt gamma-ray component of the neutron beams, which is mainly produced by the neutron capture reaction of hydrogen in the pool water in the new neutron beam ports. Figure 1 shows the 3D AutoCAD® drawings of the new core-moderator assembly design which provides the optimal neutron beam output to the beam port facilities. The only drawback of the new assembly design is the restriction of the cross-flow entering the core from the sides by the new moderator tank.

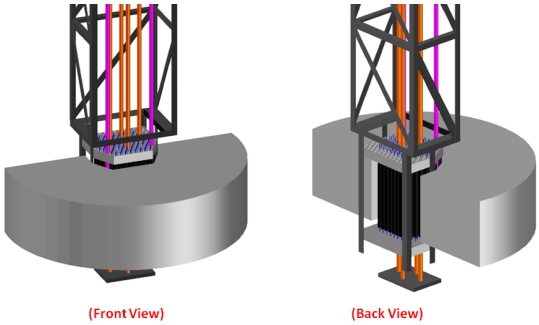

FIGURE 1: AutoCAD® drawings of the new core-moderator assembly design proposed and neutronically optimized for the PSBR.

The effect of the cross-flow on cooling the reactor core is significant in the existing core-moderator assembly as stated in several studies, which are summarized as follows. The bulk fluid temperature profile was first measured by Haag and Levine in four selected flow channels, noted as channels L, M, N, and P, going from the inner to the outer channels of the reactor core in core loading 14 (1971) [5]. A considerable decrease in the bulk fluid temperature was observed above the three-quarters in length of the active fuel rod in all four flow channels and this was noted as an indication of the effectiveness of the cross-flow on cooling the reactor core. Later, Gougar showed that approximately 90% of the coolant is entering the core from the upper side as a result of the cross-flow [6]. In that experiment, the cross-flow was restricted by covering the reactor core with rectangular-shaped shrouds and the fuel temperatures inside the instrumented fuel rods were monitored in the reactor's console. As a result, a

[1] Radiation Science and Engineering Center, The Pennsylvania State University, University Park, PA 16802
[2] Department of Mechanical and Nuclear Engineering, The Pennsylvania State University, University Park, PA 16802

considerable increase in the fuel temperature was reported. Finally, Chang performed a computational fluid dynamics (CFD) simulation of the PSBR by using FLOW3D code and implementing a porous medium approach [7]. The important outcome of this study is that the total flow rate from the sides of the core (cross-flow) was predicted to be ten times higher than the total flow rate entering from the bottom of the core (axial-flow). All of these studies confirm that the PSBR with its current core-moderator assembly design is mainly cooled by a strong cross-flow.

The moderator tank in the new design reduces the cross-flow and alters the flow geometry on the core periphery. This may adversely affect the heat transfer from the cladding to the bulk fluid and may increase the bubble nucleation rate. The major concern in the new PSBR design is the possible shift of the current flow regime (subcooled nucleate boiling) to nucleate boiling, in which the bulk fluid temperature is at saturation. The PSBR's safety limitations set the maximum fuel temperature to 1150 ^{o}C during steady-state operation of the reactor. The maximum fuel cladding outer temperature does not exceed 500 ^{o}C and clad integrity is maintained if the fuel temperature is lower than 1150 ^{o}C. This study will investigate the operating conditions of the new PSBR core-moderator assembly design by considering these thermal-hydraulics safety limits.

CFD Modeling

The thermal-hydraulics analysis of the PSBR was previously performed by using two different computational approaches: (1) Subchannel analysis with COBRA (COolant Boiling in Rod Arrays) and COBRA-TF (Two Phase) codes [6][8] and (2) CFD modeling using the FLOW-3D code and a porous medium approach [7]. Subchannel analysis codes are mainly used for the modeling of conventional nuclear power plants. These codes can be modified, as is the case in COBRA-TF, for research reactor applications. However, the new crescent-shaped moderator tank geometry significantly perturbs the flow at the periphery of the core and subchannel analysis codes are not powerful enough to model this complexity. CFD modeling with a porous medium approach is preferred for the complex geometries, but the main drawback is the correct formulation of momentum and heat transfer sources considering the effect of boiling in complex flow geometries. Therefore, a CFD model with all geometrical complexities is required to estimate the thermal hydraulics performance of the new PSBR design. Fine meshing is required to obtain accurate solutions, but computational time inversely changes with mesh size. In this study, the thermal-hydraulics analysis of the new PSBR design was achieved by using the ANSYS Fluent CFD code, which provides simultaneous computation of two-phase momentum and energy equations and density driven flow by solving the mass, momentum, energy and associated turbulence equations for both liquid and vapor phases separately [9].

The CFD simulation approach in this study is to model all of the flow details with a large number of computational meshes. The model geometry consists of the new reactor core-moderator assembly in the reactor pool. In order to reduce the computational time in the Fluent CFD simulation, the beam ports and the tower design were ignored since the focus of the study is to investigate the flow conditions within the new core-moderator assembly. A reference core with loading pattern 53H, which went critical in May 2009, was used in the simulations. In this core loading, there are 102 fuel rods, 4 control rods, and 2 dry tubes that are vertically aligned in hexagonal arrays. The TRIGA fuel and control rod designs are shown in Figure 2. The heat transfer inside the fuel rods from the fuel meat to the coolant were ignored for two reasons: (1) an excessive number of fuel rods increases the number of computational cells and, hence, the computational time, and (2) the physical and thermal properties of the gap region are not well known and drastically change between the fuel rods due to their different burnup histories. Therefore, the CFD modeling approach used in this study was to directly apply the amount of heat generated in the fuel section to the coolant. The heat generation rate in each fuel rod is estimated by the TRIGSIMS burnup code, which periodically calculates the depleted fuel compositions at five axial sections of the fuel rods since 1965 [7]. This approach is reasonable because the safety limits of the PSBR were analyzed under steady-state conditions at 1-MW full power. The burnup dependent heat flux values on the fuel claddings' outer surface (q") were calculated by using the burnup dependent local power calculated by the TRIGSIMS code with the following relation:

$$q'' \left[\frac{\text{Watt}}{\text{m}^2}\right] = \frac{\dot{Q}\,[\,\text{Watt}]}{2\pi r_c H} \qquad (1)$$

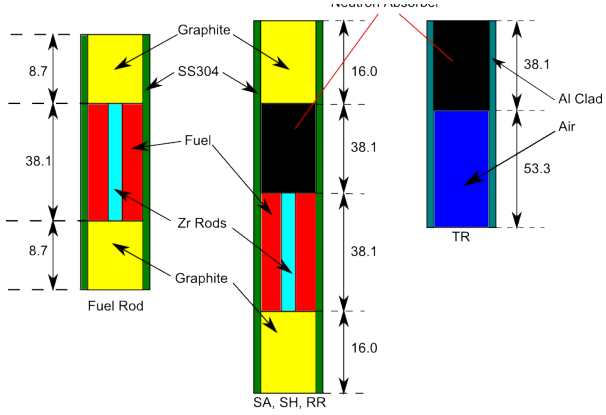

FIGURE 2: The design features of TRIGA fuel and control rods (all units are in cm).

where r_c is the outer surface radius of the clad (1.83cm) and H is the axial height of each fuel rod section (7.62 cm).

The heat is transferred from the fuel rod to the water coolant via thermal conduction in the boundary layer, the natural convection, and the subcooled nucleate boiling at the fuel claddings' outer surface in the PSBR. The natural convection is driven by the coolant density difference, which is a function of the temperature gradient in the flow channels. The density difference due to the temperature gradient is determined by the thermal expansion coefficient β, which can be written as:

$$\beta = -\frac{1}{\rho}\left(\frac{\partial \rho(T)}{\partial T}\right)_p \quad (2)$$

The difference in density causes the buoyancy force to act on the coolant. This buoyancy force creates an additional component in the momentum and energy equations, which promotes convection via a local density change.

Subcooled boiling is expected during operating conditions in the PSBR [5]. When the temperature at the claddings' outer surface exceeds the saturation temperature of the water, bubbles are likely to nucleate on the cladding surface. The bubble creation near the wall requires sufficient surface tension forces to sustain it. Therefore, the bubble nucleation is a strong function of the claddings' surface roughness. However, the bubble nucleation due to this roughness is not considered in this study. On the fuel cladding, bubble nucleation starts at the Onset of Nucleate Boiling (ONB) point where a sufficient amount of wall superheat is reached. The subcooled boiling region and bubble densities are highly dependent on the reactor's operating conditions. The subcooled nucleate boiling in an upward flow between vertical channels can be categorized into "highly subcooled" and "low subcooling" regions by considering the system pressure since the size and velocity of the bubbles are a strong function of the system pressure [10]. At low pressure applications, i.e. research reactors operating near atmospheric pressure, the highly subcooled region just after the ONB point is characterized by small bubbles restrained to a thin, long and almost flat two-phase layer near the vertical heated wall. The void fraction significantly increases after Onset of Significant Void (OSV) point. The OSV point represents the transition from a highly to low subcooling region. The two-phase layer in the low subcooling region is thicker and the bubbles are larger compared to the highly subcooled region [10-12]. The bubbles in this region can slide along the heated walls and eventually depart from the heated walls. These bubbles can move further away from the heated fuel elements to a subcooled liquid at low pressure.

The presence of subcooled boiling in flow channels dictates multiphase thermal-hydraulics modeling in the PSBR geometry. ANSYS Fluent provides a two-fluid model based on the Eulerian multiphase flow formulation. In this model, conservation of momentum and energy equations are solved separately for each phase by two-sets of averaged transport equations. Both liquid and vapor phases are treated as incompressible Newtonian fluids. However, Eulerian formulation is legitimate when both phases are present in the flow. Since a second vapor phase is created by the subcooled nucleate boiling in the PSBR core, a boiling model has to be defined in the CFD simulation. ANSYS Fluent provides the Rensselaer Polytechnic Institute (RPI) wall boiling model for the subcooled nucleate boiling, which was employed in this study [11]. Besides the boiling model, additional closure relations are required to close the averaged flow equations for mass, momentum, and energy. Detailed information about the two-fluid model is described by Ishii and Hibiki [12] and discussed in later sections. The general features of the applied CFD model to the problem are given in Table 1.

TABLE 1: General features of the applied models in the ANSYS Fluent CFD simulation

Feature	Model
Solver	Pressure-based Segregated
Formulation	Transient
Multiphase	Eulerian with RPI Boiling Model
Turbulence Approach	k-omega
Turbulence Multiphase Model	Mixture
Near-wall Treatment	SST
Pressure Interpolation Scheme	Body-force Weighted
Pressure Velocity Coupling	Phase Coupled Simple
Spatial Discretization	Second Order Upwind
Temporal Discretization	Second Order Upwind
Geometry	3-dimensional, PSBR core
Walls	No-slip
Time-Step Size	0.01

Computational Mesh

The ANSYS Gambit meshing tool (v2.4) was employed to generate the computational mesh for the model geometry. Approximately 22-million hybrid meshes with unstructured and structured grids in the pool region and structured grids in the fuel rod channels were generated for the CFD model, shown in Figures 3 and 4. In the core region, structured meshes were preferred and the mesh structure was very fine in order to include the effect of velocity and thermal boundary layers to the thermal-hydraulics calculation. Mesh

independence of the simulation was achieved by making the CFD calculations in eight subchannels within ten fuel rods close to the center of the reactor core. The mesh structure which provided the independent solution in this calculation was then applied to all the flow channels throughout the core. The meshing and CFD simulations were completed in the Lion-LSP high-performance computing (HPC) cluster of The Pennsylvania State University.

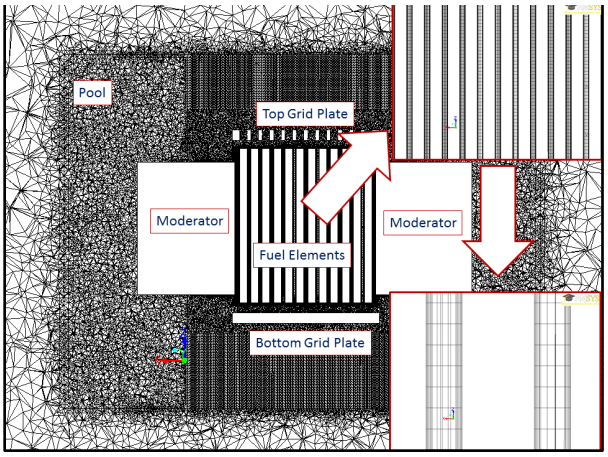

FIGURE 3: Sketch of the geometry and numerical grid for computational domain shown along an axial plane at the center of the core

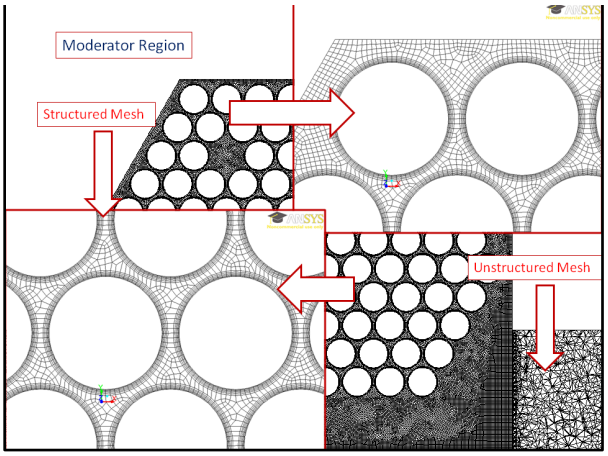

FIGURE 4: Mesh structure for the computational domain in the core and pool regions

Description of Models

Continuity, momentum, and energy equations derived for each phase of the multiphase flow in ANSYS Fluent are expressed with the following equations. The continuity equation for phase-k is:

$$\frac{\partial \rho_k \alpha_k}{\partial t} + \nabla.(\rho_k \alpha_k \vec{v}_k) = \sum_{k=1}^{n} \Gamma_{kl} \qquad (3)$$

where the subscripts k and l denote the phases, α_k is the volume fraction of each phase, and Γ_{kl} is the volumetric mass exchange between phases k and l.

The momentum conservation equation for phase-k is:

$$\frac{\partial}{\partial t}(\rho_k \alpha_k \vec{v}_k) + \nabla.(\rho_k \alpha_k \vec{v}_k \vec{v}_k) = -\alpha_k \nabla P + \nabla.[\alpha_k(\tau_k + \tau_k^T)] + \rho_k \alpha_k \vec{g} + M_{ki} - \tau_{ki}.\nabla\alpha_k + (p_{ki} - p_k)\nabla\alpha_k \qquad (4)$$

where interphase momentum exchange, velocity, shear and pressure are denoted by M_{ki}, v_{ki} and p_{ki}, respectively. τ_k is the viscous shear stress on phase k and τ_k^T is the bubble-induced turbulence terms defined by a correlation proposed by Sato, et.al. in Fluent [13]. In the preceding equation, the momentum exchange term is defined by the following interfacial forces: drag force, lift force, wall lubrication force, and turbulence dispersion force. It is crucial to select the proper models for the interfacial forces for the two-phase flow modeling in Fluent. There are several correlations that exist to model these forces, which depend on several factors including relative velocity, bubble diameter, near wall mesh size, void fraction, etc. However, the flow conditions within the PSBR flow channels are not known precisely. Therefore, the selection of interfacial force models was performed with the investigation of similar studies in the literature. Drag force is due to the velocity and density differences between the continuous (liquid) and dispersed (bubbles) phases. It tends to slow down the vapor phase and speed up the liquid phase in order to decrease relative drift between the phases. In this study, the drag force was modeled according to a correlation given by Schiller and Naumann, which is highly accurate for low velocity flows [14]. The lift force pushes the small bubbles to the wall and the lift coefficient for the lift force on the liquid phase was defined by a correlation proposed by Moraga, et.al. [15]. The turbulent dispersion force describes the effect during diffusion of the vapor phase caused by turbulent eddies in the liquid phase. Fluent provides a general correlation for this force based on Simonin and Violett's study [16]. Similar to the turbulent dispersion force, the default formulation provided by Fluent was employed for modeling of the virtual mass force between the phases.

The energy equation is defined in terms of enthalpy as:

$$\frac{\partial}{\partial t}(\rho_k \alpha_k h_k) + \nabla.(\rho_k \alpha_k \vec{v}_k h_k) = -\alpha_k \left(\frac{\partial P_k}{\partial t} + \vec{v}_k.\nabla P_k\right) + \overline{S}_k:\nabla.\vec{v}_k + R_k - \nabla.\vec{q}_k + \sum_{k=1}^{n} \gamma_{ki}(T_i - T_k) + \dot{m}_{ki}(h_k - h_{ik}) \qquad (5)$$

where γ_{ki} denotes the interphase heat transfer coefficient defined by the Ranz-Marshall correlation in the Fluent model [17].

Interfacial area concentration defines the area between the phases per unit mixture volume. It represents the change in the interfacial area between the phases. The transport equation for the interfacial area concentration is written with the interfacial area concentration χ_p, the mass transfer rate to the gas phase per unit mixture volume $\dot{m}_g$, the gas volume fraction a_g, the coalescence sink term S_{RC}, the wake entrainment term S_{WE}, and the breakage source term S_{TI}. Fluent provides three sets of empirical correlations to model the source and sink terms: the Hibiki-Ishii model 18], the Ishii-Kim model [19] and the Yao-Morel model [20]. In this study, coalescence and breakage source terms were modeled with the Hibiki-Ishii formulation, the nucleation rate on the heated wall was defined by the Yao-Morel model with a critical Weber number set to six, the Ishii-Kim model was employed to model the dissipation rate, and the diameter of the bubbles was modeled by the Sauter-mean diameter correlation [21]. Detailed information about these models as well as interfacial momentum forces is given in reference [9].

The RPI wall boiling model was developed by Kurul and Podowski [11] and it is implemented by a UDF in Fluent. In this model, the heat flux from the heated wall to subcooled fluid is partitioned into three components:

$$q'' = q''_{1\phi} + q''_{Q} + q''_{e} \quad (6)$$

where $q''_{1\phi}$ is the single-phase convective heat flux, q''_{Q} denotes the quenching heat flux and the q''_{e} is evaporative heat flux. Single phase convective heat flux is used to define the heat transfer from the heated wall to the liquid phase only. The single-phase convective heat flux in the RPI model is calculated with:

$$q''_{1\phi} = h_{1\phi}(T_W - T_l)(1 - A_b) \quad (7)$$

In the preceding equation, A_b denotes the bubble influence area which defines the area covered by the bubbles on the heated wall, $h_{1\phi}$ is the single phase heat transfer coefficient, T_w is the wall temperature, and T_l is the local liquid temperature in the near-wall computational cell. In the RPI wall boiling model, the bubble influence area is determined as:

$$A_b = \min\left[1, K\frac{N_W \pi d_{bw}^2}{4}\right], \quad (8)$$

where K is an empirical constant, which determines the size of the bubble influence area, d_{bw} stands for the bubble departure diameter, and N_W is the active nucleation sites per unit wall area. In Fluent, an empirical constant based on a Del-Valle and Kenning study was used to model the K constant [22]. For turbulent flow, the single-phase heat transfer coefficient $h_{1\phi}$ is determined by using the local Stanton number, which is the ratio of heat transferred into the liquid to the heat capacity of the liquid.

The quenching heat flux defines the heat transfer from the heated wall to the continuous liquid phase that periodically fills the volume vacated by the bubbles departing or condensing within a period. In the RPI model, the quenching heat flux is determined as:

$$q''_{Q} = \frac{2k_l}{\sqrt{\pi T/f}}(T_W - T_l), \quad (9)$$

where k_l is the conductivity of the liquid phase, T is the periodic time between the beginning and the departure of a bubble, and f is the bubble nucleation frequency. T was set to 1 in the CFD model and the bubble departure frequency as the ratio of the terminal rise velocity to the bubble departure diameter was defined by the Cole correlation [23]. The RPI model defines the evaporative component of the wall heat flux, which is needed to generate vapor bubbles as:

$$q''_{e} = V_d N_W \rho_v h_{fv} f, \quad (10)$$

where V_d is the volume of the maximum diameter of bubbles at the departure (d_{bw}), N_W is the nucleate site density, f is the bubble departure frequency, ρ_v is the vapor density, and h_{fv} is the latent heat of evaporation. In this study, the bubble departure diameter and nucleation site density were modeled by using the Tolubinski-Kostanchuk [24] and Kocamustafaogullari-Ishii correlations [25], respectively.

In the RPI model, the vapor temperature is assumed to be at saturation temperature. The critical heat flux conditions are not expected in the new PSBR core-moderator assembly design. Thus, this assumption is applied in the CFD analysis. Heat transfer occurs from vapor to liquid phase due to the condensation in coolant channels after bubble detachment from the fuel rod. The interfacial heat transfer to the liquid phase is defined by using the following relation:

$$\dot{q}_{lt} = A_{it} h_{lt}(T_{sat} - T_l), \quad (11)$$

where A_{it} is the interfacial area per unit volume and h_{lt} is the interfacial heat transfer coefficient based on the Nusselt number defined by the Ranz-Marshall correlation [17].

Results and Discussion

The Fluent CFD simulation of the new PSBR design was compared with two sets of experimental data [5] and Cobra-TF simulation results for the bulk fluid temperature profile in the hot channel of the existing PSBR design. The thermal-hydraulics performance of the new design was evaluated based on this comparison. In order to understand the operating conditions of the new reactor design, the CFD simulation results are given for radial and axial flow paths at different regions of the new core-moderator

assembly along with the contours of bulk fluid velocity, temperature and void fraction in the hot channel at maximum power (1 MW). The local power distribution in the reactor core is given in Figure (5). Notably, instrument rod 16 (I-16) was found to be the hottest fuel rod in the core and thus the estimated hot channels in both the existing and new designs were unchanged.

In Figures 6 and 7, the radial and axial flow paths colored by velocity magnitude at the center of the new core geometry are given. The new moderator tank causes a substantial decrease in the cross-flow area and results in a secondary flow entering into the core, shown in Figure 6. The axial-flow distribution along the flow channels shown in Figure 7 represents symmetrical flow distribution in the core and the laminar-to-turbulent flow transition at the entrance of the channel. The radial-flow enhances radial-mixing in the core and thus the local heat transfer conditions.

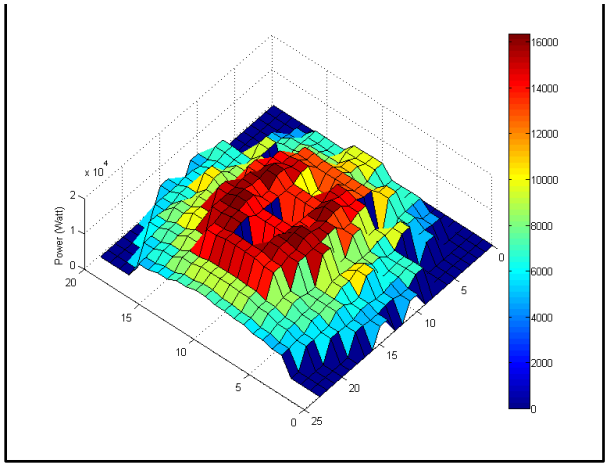

FIGURE 5: The local power distribution in the reactor core at 1 MW. The local power distribution was calculated using the TRIGSIMS code [26].

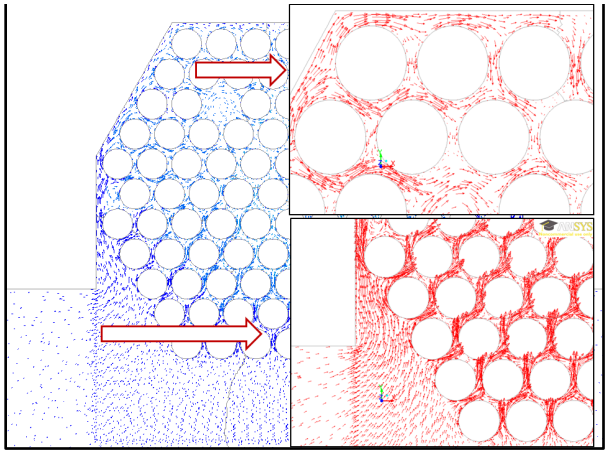

FIGURE 6: Radial flow paths at the center of the new core-moderator assembly design

Similarly, the flow symmetry in the new reactor core was clearly observed in the radial velocity profile.

The velocity, temperature, and void fraction distributions in the estimated hot channel at the center of the core are given in Figures 8, 9, and 10, respectively. As expected, the velocity magnitude is smaller in the thermal and velocity boundary layer, which are reasonably well defined as seen in Figure 8. Therefore, the bulk fluid temperature close to the heated fuel rods is higher. As seen in Figure 10, nucleated bubbles detach from the fuel cladding. However, they are condensed within the boundary layer before reaching the subcooled bulk fluid. Therefore, vapor bubbles do not affect the bulk fluid temperature. However, heat transfer improves in close vicinity to the bubble layer formed within the boundary layer. The Fluent model predicted the maximum liquid temperature as 88 ^{o}C, which was observed at the exit of the hot channel on top of the core.

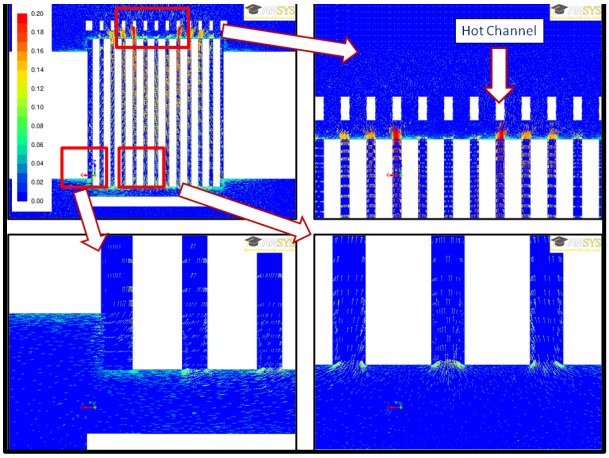

FIGURE 7: Axial flow paths colored by velocity magnitude (m/s) in a vertical plane crossing the hot channel in the new core-moderator assembly design.

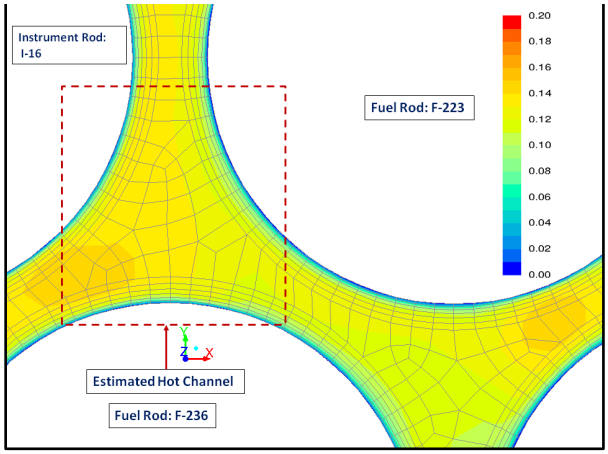

Figure 8: The contours of the bulk fluid velocity magnitude profile (m/s) at the center of core-moderator assembly and in the hot channel.

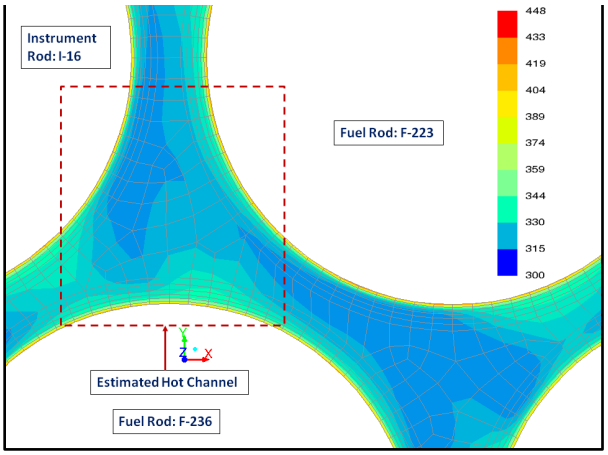

FIGURE 9: The contours of the bulk fluid temperature profile (Kelvin) at the center of core-moderator assembly and in the hot channel.

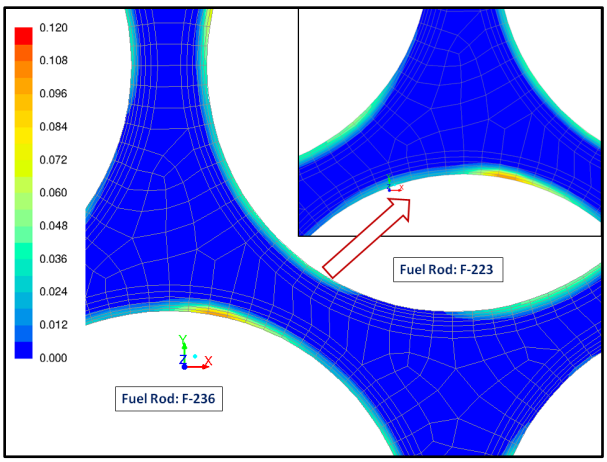

FIGURE 10: The contours of the void fraction profile at the center of core-moderator assembly and in the hot channel.

Table 2 compares the bulk fluid temperatures estimated by the Fluent CFD analysis to experimental and Cobra-TF simulation results at two axial locations. The experimental temperature measurements were obtained by using a thermocouple contained in an aluminum tube with a 0.25" outer diameter. This tube considerably decreases the cross-sectional flow area of the channel while the same amount of heat is transferred into the fluid. This makes the temperature measurements and the comparison unreliable. Therefore, the thermal-hydraulics performance of the new PSBR design was evaluated by relying on the Cobra-TF simulation results obtained in the existing design. This indicated that an 11 ^{o}C increase would be observed in the bulk fluid temperature at two axial locations shown in the Table 2.

Another comparison was made by using the measured temperature profile in four selected flow channels (L, M, N and P) in core loading-14 [5]. The compared bulk fluid temperature profiles are shown in Figure 11. The main observation in this figure is the steady increment of the bulk fluid temperature in the flow channels of the new PSBR core. In the measurements, a considerable decrease was observed for the bulk fluid temperature after three-quarters of active length of the fuel rods because of the cross-flow. Since the new moderator tank shape significantly decreases the cross-flow, a steady increase was observed in the bulk fluid temperature in the flow channels of the new PSBR design. But, the bulk fluid temperature is still well below the saturation temperature of the water, which is 111 ^{o}C in the core.

The average cladding outer temperature of the instrument rod-16 (I-16) was predicted as 175 ^{o}C by the Fluent CFD simulation. The maximum fuel temperature of I-16 was determined by using this cladding outer temperature and the heat generation rate estimated by the TRIGSIMS fuel management code in the following relation [27]:

$$T_{fuel} - T_c = \frac{q''' r_f}{2}\left[\frac{r_f}{2k_f} + \frac{1}{h_g} + \frac{t_c}{k_c}\right] \quad (12)$$

where q''' is the volumetric heat generation rate in the unit of W/m^3, r_f is the fuel radius, k_f is the thermal conductivity of the fuel, h_g is the gap heat transfer coefficient, t_c is the cladding thickness, and k_c is the thermal conductivity of the cladding.

TABLE 2: The comparison of the Fluent CFD-calculated bulk fluid temperatures in the new PSBR design with the experimental and Cobra-TF simulation results at two axial locations of the estimated hot channel.

Axial Location (cm)	Existing Reactor Core Design with Loading-53H		New Reactor Core Design with Loading-53H
	Measured Temperature (^{o}C)	Cobra-TF-Estimated Temperature (^{o}C)	Fluent CFD-Estimated Temperature (^{o}C)
19.05 (core center)	58.00	54.00	65.42
31.12	59.30	66.00	78.88

The volumetric heat generation rate in the I-16 was determined by the TRIGSIMS code as $5.33x10^7$ W/m^3. The gap heat transfer coefficient was estimated by using the correlation provided by General Atomics [28]:

$$h_g = 0.0239q^2 - 1.4372q + 1593.1 \quad (13)$$

where q is the reactor power in kW. By using this formula, h_g was determined to be 9228 W/m^2/K in I-16 for 1 MW power operation.

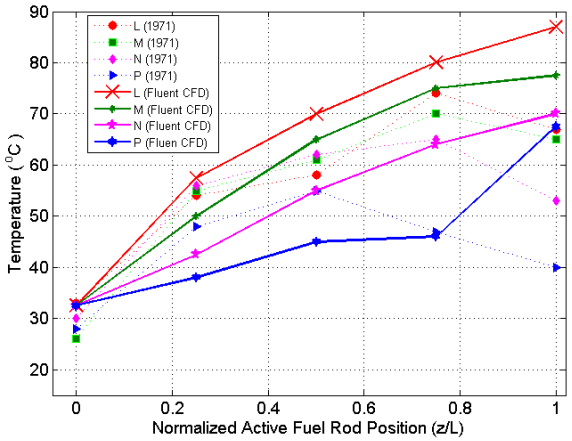

FIGURE 11: Comparison of the bulk fluid temperature profiles in four selected flow channels (L, M, N and P) between experimental results in core loading-14 [5] and the Fluent CFD simulation results in the new core-moderator assembly design.

For a typical TRIGA fuel rod, thermal conductivities of the fuel and cladding are suggested by General Atomics to be 18 W/m/K and 14 W/m/K, respectively [29]. The cladding thickness was calculated by assuming that the gap thickness would be 0.0025 cm in the fuel rods as predicted by sensitivity studies using the Cobra-TF code [8]. By employing the TRIGSIMS estimated and the General Atomics suggested thermal properties of the TRIGA fuel rod, the maximum fuel temperature in I-16 was estimated at 482 ^{o}C, which is considerably lower than the measured fuel temperature of 540 ^{o}C. The difference between these two results is mainly caused by the gap heat transfer coefficient and thermal conductivity of the fuel employed in the calculations. The data provided by General Atomics are just recommended values and only given as an estimate of actual values. General Atomics recommends three hypotheses which differ by ~50%. However, the gap heat transfer coefficient and the fuel thermal conductivity significantly change as a function of burnup during the lifetime of the fuel rods. Fuel thermal conductivity decreases as the burnup of the fuel rod increases. Although the fuel temperature in I-16 is expected to be higher than the measured value, it will still be well under the safety limit of the PSBR.

Conclusion

In this study, it is verified by ANSYS Fluent CFD simulations that the new core-moderator assembly design proposed for the PSBR will operate under safety limits. The CFD model is based on a two-fluid Eulerian formulation of mass and momentum, a two-phase mixture turbulence model, and an energy equation for the liquid phase. A large number of computational meshes were used to fully capture all the flow details in the channels. Although this approach was computationally expensive, it was highly successful in calculating very detailed velocity, temperature, and void fraction distributions in the new core-moderator assembly design. The Eulerian multiphase flow formulation with the RPI wall boiling model gave reasonably accurate results to determine the bubble nucleation on the fuel rods cladding. Although bubble nucleation and detachment were observed within the thermal boundary layer, the subcooled liquid flow was not affected by the presence of the bubbles. Bubbles only enhanced the heat transfer from the fuel rod cladding to the subcooled liquid. Considering the loss of cooling due to the reduction in the cross-flow rate by the crescent-shaped moderator tank, only an 11-^{o}C increment was observed in the bulk fluid temperature of the new PSBR design. In addition, the predicted fuel temperature in I-16 is well below the safety limit. This shows that the new design is mainly cooled by axial-flow contrary to the existing design. Additionally, the significance of the cooling by the cross-flow in the reactor core is another important outcome of this study. The CFD simulation provides useful information for the neutronic modeling. It is possible to calculate the reactivity feedback effects in the new PSBR design for the temperature and void fraction. However, the CFD results should be verified with further experimental results and different simulation approaches.

Acknowledgements

This work is supported by the Radiation Science and Engineering Center at the Pennsylvania State University, and represents work submitted as part of the Ph.D. dissertation of D. Uçar. The authors are very thankful to all RSEC personnel, Dr. Seungjin Kim, and Mahmut Nedim Cinbiz for their invaluable contributions and comments in the completion of this study.

References

1. J. S. Butler, “Instrument Selection and Layout for the Penn State Neutron Beam Hall Expansion,” M.Sc. thesis, The Pennsylvania State University, University Park, PA, 2006.
2. B. Sarikaya, “Modeling of Existing Beam Port Facility at Penn State Breazeale Reactor By Using MCNP5,” M.Sc. thesis, The Pennsylvania State University, University Park, PA, 2004.
3. K. B. Bekar, “Modular Optimization Code Package: MOZAIK,” Ph.D. thesis, The Pennsylvania State University, University Park, PA, 2009.
4. D. Uçar, “Modeling and Design of A New Core-Moderator Assembly and Neutron Beam Ports for the Penn State Breazeale Reactor (PSBR),” Ph.D. Dissertation, The Pennsylvania State University, University Park, PA, 2013.
5. J. A. Haag and S. H. Levine, “Thermal Analysis of The Pennsylvania State University Breazeale Nuclear Reactor,” Nucl Technol. **19**, 6 (1973)

6. H. D. Gougar, “Development and modeling of coolant flow control in the Penn State Breazeale Reactor,” Ph.D. Thesis, The Pennsylvania State University, University Park, PA, 1997.
7. E. J. Chang, “Thermal-hydraulic modeling of the Pennsylvania State University Breazeale Nuclear Reactor (PSBR),” Ph.D. Thesis, Pennsylvania State University, University Park, PA, 2005.
8. V. Karriem, “PSBR Core Design Studies of the D_2O Tank Design and New LEU Fuel Utilization,” M.Sc. thesis, The Pennsylvania State University, University Park, PA, 2011.
9. “ANSYS Fluent Theory Guide Release 14.0.” ANSYS, Inc., Nov-2011.
10. J. G. Collier, Convective boiling and condensation. McGraw-Hill, USA (1981).
11. N. Kurul and M. Z. Podowski, “On the modeling of multidimensional effects in boiling channels,” in In Proceedings of the 27th National Heat Transfer Conference, Minneapolis, Minnesota, USA (1991).
12. M. Ishii and T. Hibiki, Thermo-fluid Dynamics of Two-Phase Flow. Springer, USA (2005).
13. Y. Sato, M. Sadatomi, and K. Sekoguchi, “Momentum and heat transfer in two-phase bubble flow—I. Theory,” Int. J. Multiph. Flow **7**, 167–177 (1981).
14. L. Schiller and Z. Naumann, A drag coefficient correlation, Z. Ver Deutsch. Ing. **77**, 318 (1935).
15. B. F. J. Francisco J. Moraga, “Lateral forces on spheres in turbulent uniform shear flow,” Int. J. Multiph. Flow, **25**, 1321–1372 (1999).
16. C. Simonin and P. L. Viollet, “Predictions of an Oxygen Droplet Pulverization in a Compressible Subsonic Coflowing Hydrogen Flow, Numerical Methods for Multiphase Flows,” FED **91**, 65–82 (1990).
17. M. E. Ranz and W. R. Marshall, “Evaporation from drops: Part I,” Chem. Eng. Prog. **48**, 141–146 (1952).
18. M. I. T. Hibiki, “One-group interfacial area transport of bubbly flows in vertical round tubes,” Int. J. Heat Mass Transf. **43**, 2711–2726 (2000).
19. Q. Wu, S. Kim, M. Ishii and S. G. Beus, “One-group interfacial area transport in vertical bubbly flow,” Int. J. Heat Mass Transf. **41**, 1103–1112 (1998).
20. C. M. Wei Yao, “Volumetric interfacial area prediction in upward bubbly two-phase flow,” Int. J. Heat Mass Transf. **47**, 307–328 (2004).
21. J. Sauter, Determining size of drops in fuel mixture of internal combustion engines, Washington, D.C. : National Advisory Committee for Aeronautics, USA (1926).
22. V. H. D. Valle and D. B. R. Kenning, "Subcooled Flow Boiling at High Heat Flux," Int. J. Heat Mass Transf. **28**, 1907-1920 (1982).
23. R. Cole, “A photographic study of pool boiling in the region of the critical heat flux,” AIChE J. **6**, 533–538 (1960).
24. V. I. Tolubinski and D. M. Kostanchuk, “Vapour bubbles growth rate and heat transfer intensity at subcooled water boiling,” 4th International Heat Transfer Conference, Paris, France (1970).
25. G. Kocamustafaogullari and M. Ishii, “Interfacial area and nucleation site density in boiling systems,” Int. J. Heat Mass Transf. **26**, 1377–1387 (1983).
26. C. Tippayakul, K. Ivanov, and C. Frederick Sears, “Development of a practical Monte Carlo based fuel management system for the Penn State University Breazeale Research Reactor (PSBR),” Ann. Nucl. Energy **35**, 539–551 (2008).
27. N. E. Todreas and M. S. Kazimi, Nuclear Systems Volume I. CRC Press, USA (2010).
28. General Atomics, “Safeguards Summary Report for the New York University TRIGA Mark I Reactor,” San Diego, (GA-9864), 1970.
29. General Atomics, “TRIGA Mark III Reactor Description,” General Atomics, Division of General Dynamics, 4339, (1963).